



Published in final edited form as:

J Neural Eng. 2016 December ; 13(6): 066013. doi:10.1088/1741-2560/13/6/066013.

OptoZIF Drive: a 3D printed implant and assembly tool package for neural recording and optical stimulation in freely moving mice

David S. Freedman^{#1,*}, Joseph B. Schroeder^{#2}, Gregory I. Telian^{2,*;3}, Zhengyang Zhang², Smrithi Sunil², and Jason T. Ritt²

¹ Boston University, Center for Neuroscience

² Boston University, Department of Biomedical Engineering

³ University of California Berkley, Department of Molecular and Cell Biology and the Helen Wills Neuroscience Institute

These authors contributed equally to this work.

Abstract

Objective—Behavioral neuroscience studies in freely moving rodents require small, light-weight implants to facilitate neural recording and stimulation. Our goal was to develop an integrated package of 3D printed parts and assembly aids for labs to rapidly fabricate, with minimal training, an implant that combines individually positionable microelectrodes, an optical fiber, zero insertion force (ZIF-clip) headstage connection, and secondary recording electrodes, e.g. for electromyograms (EMG).

Approach—Starting from previous implant designs that position recording electrodes using a control screw, we developed an implant where the main drive body, protective shell, and non-metal components of the microdrives are 3D printed in parallel. We compared alternative shapes and orientations of circuit boards for electrode connection to the headstage, in terms of their size, weight, and ease of wire insertion. We iteratively refined assembly methods, and integrated additional assembly aids into the 3D printed casing.

Main Results—We demonstrate the effectiveness of the OptoZIF Drive by performing real time optogenetic feedback in behaving mice. A novel feature of the OptoZIF Drive is its vertical circuit board, which facilitates direct ZIF-clip connection. This feature requires angled insertion of an optical fiber that still can exit the drive from the center of a ring of recording electrodes. We designed an innovative 2-part protective shell that can be installed during the implant surgery to facilitate making additional connections to the circuit board. We use this feature to show that facial EMG in mice can be used as a control signal to lock stimulation to the animal's motion, with stable EMG signal over several months. To decrease assembly time, reduce assembly errors, and improve

Corresponding Author Jason Ritt, Boston University, Department of Biomedical Engineering, 44 Cummington Mall, Boston, MA 02215, jritt@bu.edu.

*DSF was affiliated with Boston University, Center for Neuroscience, JBS and GIT were affiliated with Boston University, Department of Biomedical Engineering when this work was completed.

repeatability, we fabricate assembly aids including a drive holder, a drill guide, an implant fixture for microelectrode “pinning”, and a gold plating fixture.

Significance—The expanding capability of optogenetic tools motivates continuing development of small optoelectric devices for stimulation and recording in freely moving mice. The OptoZIF Drive is the first to natively support ZIF-clip connection to recording hardware, which further supports a decrease in implant cross-section. The integrated 3D printed package of drive components and assembly tools facilitates implant construction. The easy interfacing and installation of auxiliary electrodes makes the OptoZIF Drive especially attractive for real time feedback stimulation experiments.

Introduction

Behavioral neuroscience often requires the ability to record neural activity in freely moving animals by implanting light-weight devices. The increasing availability of optogenetic tools for studying specific neural circuits [1–5] makes the integration of optical fibers for open and closed-loop manipulation of neural firing an important design criteria. The challenge of building neural interfaces is exacerbated when working at rodent scale (e.g. compared to primates with larger, fixed electrode arrays and headstages), especially in mice, that are about one tenth the size of rats. However, mice are heavily favored for genetic approaches for targeted optogenetic expression, making the continuing development of light-weight chronic recording technology an important technical problem. A well developed and ubiquitous design features a ring of electrodes (often 2-channel stereotrodes or 4-channel tetrodes) that can be independently vertically positioned by adjusting screws (microdrives) in an encasing “hyperdrive” [6,7].

3D printed versions have been used in rats [8,9] and mice [10], with the latter also incorporating an optical fiber for simultaneous neural recording and optogenetic stimulation. More recent work has made significant strides in weight reduction while at the same time allowing for increased flexibility and higher channel counts [11–13]. There are now a wide variety of design approaches. Examples include lightweight motorized drives for improvements in positioning precision over manual screw adjustments [14–17], “optrode” technologies that seek to bring the stimulation source into close proximity with the recording electrodes [18–20], microelectrode arrays with integrated optical fibers [21,22], and silicone probes that incorporate micro scale LEDs [23]. Other approaches sacrifice size and repositionability to make high channel count arrays for mice [24], or focus on incorporating wireless technology to remove the need for a tether/commutator during behavioral tasks [25,26]. Each of these devices accepts trade-offs to optimize features important to a particular research need. Some devices are labor intensive to assemble, may have poor reproducibility from build to build, and/or require specialized knowledge or equipment.

The OptoZIF Drive presented here facilitates assembly by 3D printing a package of not only drive parts, but also assembly guides and tools for straightforward construction. The drive is light-weight (~3 g), supports a fiber-optic channel and six adjustable drives, and can be assembled with minimal training. A novel feature of the OptoZIF Drive is that it is designed for the ZIF-clip® system used by Tucker-Davis Technologies. Zero insertion force (ZIF)

connectors snap over the hyperdrive electrical connector, without requiring tension between the headstage and drive during attachment and detachment (contrasted, for example, with the common Omnetics connectors used in NeuraLynx and Plexon systems). This process lowers the risk of drive damage and animal stress or injury, which while small on each day, can be problematic over weeks of daily recording sessions. Some existing systems use adaptors or other *ad hoc* assemblies to create a right angle between the connector and a traditionally horizontal circuit board (e.g. Tucker Davis Technologies ZCA-OMN32). We made ZIF-clip support “native” to our drive through a vertically oriented printed-circuit board (PCB) that allows direct ZIF-clip connection. An additional novel OptoZIF Drive element is a multi-part protective shell that is installed during the implant surgery to facilitate electromyography (EMG) electrode implantation; this approach is contrasted with fixed plastic cones that are usually secured to drives before implantation [10]. Together these features provide a light, low profile, flexible design for optogenetic experiments in freely moving mice.

Material and Methods

The OptoZIF Drive incorporates a number of novel innovations that build off of previously reported optoelectric hyperdrives [10] and are adapted to our experimental requirements [27]. Specifically, the implant required a vertical facing electrode interface board to reduce the height associated with ZIF-clip adapters, precise control of microelectrodes over time, an optical fiber for optogenetic stimulation, the ability to easily connect and validate the positioning of EMG electrodes during the implant surgery, and a simple and robust manufacturing process (figure 1).

Implant Fabrication Process

The drive bodies used in previous designs [10] were manufactured using a stereolithography (SLA) process to produce large batches of drives. This process frequently results in a large number of drives found to be unsuitable during the assembly process due to a variety of defects. Selective Laser Sintering (SLS) was selected as a low-cost, quick, and relatively cheap 3D printing process which allowed rapid development and iterations of the designs. The SLS process enables single drives to be manufactured quickly and cheaply. Additionally, the properties of the SLS polyamide were found to be favorable for the numerous post-processing steps (described in the supplementary material) and comparable long-term structural performance was also observed. Thus, the implant was designed to be 3D printed in single batches with the necessary supporting mechanical components 3D printed in parallel with the main implant. The main block contains the drive body, 2-part protective shell, and protective caps (figure 1(f)). In addition, the top of the block provides holders for the microdrives during assembly and grooves on the top of the main block provide length guides when cutting metal and polyimide tubes for subassemblies. Finally, we also 3D printed the distal cannula of the drive in high detail stainless steel in order to provide a consistent implant height and ensure a smooth bevel on the distal end (figure 1(b)).

Recording Electrode Configurations

The OptoZIF Drive is designed to support up to eight independently positionable microdrives. A variety of different recording configurations could be incorporated using this system- for example a single drive could be assigned to move 1 tetrode, 2 stereotrodes (i.e. fused together, but at different lengths), or 4 single electrodes. Each drive corresponds to a single polyimide guide tube that opens at the base of the drive. These guide tubes are arranged in a ring surrounding a larger polyimide tube that serves as a guide to place the optical fiber (figure 1(b), inset).

Drive Mechanism

For chronic neural recording, it is often desirable to be able to vertically reposition microelectrodes both to target specific brain regions and to optimize the quality of neural recordings. This is accomplished through an array of integrated micromanipulators that allow precise positioning of electrodes using a shuttle tube that is affixed to a “top piece” manipulated using a small control screw similar to previous designs [8,10]. OptoZIF Drive incorporates top pieces that are 3D printed along with the main drive body. As shown in figure 1(d), the shuttle tube is affixed to the microelectrodes and metal guide tubes so that turning the control screw results in a precise movement of the microelectrode. The screws have a 0.8 mm diameter and 127 threads per inch. Thus, one turn advances the screw by 200 microns. Partial rotations of ¼ turn (50 microns) or even 1/8 turn (25 microns) can be used for small electrode advancements. We used screws 0.32” (8.1 mm) in length, which provided about 6.2 mm of useable threads once the drive is assembled, giving a safe travel range of 4.0 mm through the drive body.

Vertical electrode interface board facilitates direct ZIF-clip connectivity

A recording drive's design must factor in the requirements of the recording apparatus that it will interface with. In our case, a Tucker Davis Technologies (TDT) DSP was selected for use in ongoing real time feedback experiments in part because of the flexibility offered in developing real time control algorithms. The TDT system utilizes ZIF-clip (zero insertion force) headstages that offer significant benefits for easily connecting awake animals to the recording equipment in a way that minimizes the forces on the drive and the stress experienced by the animal. Many previous drive designs featured an Omnetics connector on a horizontal EIB, requiring the use an Omnetics to ZIF adapter for use with TDT recording hardware. The adapter not only negated the benefits of the zero insertion force concept (inserting and removing the adapter requires significant force) but also nearly doubled the height of the implant, which impaired the mouse's ability to perform certain experimental tasks.

OptoZIF Drive has met this connectivity challenge by incorporating a vertically positioned EIB for direct, low-profile connection to the ZIF-clip system. A custom printed circuit board (PCB), which is 1/32” thick (0.79 mm) was made to properly use the ZIF-clip and is held in place by a dedicated receptacle on the 3D printed drive body (figure 1 (c,e)). A single EIB and absence of a connector adapter is used to reduce weight and volume, and the ZIF-Clip design includes multiple mechanical supports to prevent the ZIF-connector on the EIB from accidentally breaking during usage. To date we have had no EIBs damaged during use.

Optical fiber placement

While past designs have placed a vertical fiber directly in the center of the drive through a small hole in the EIB and adjusted the positioning of other components (such as the recording connector) to accommodate it, this strategy is contraindicated by the design features needed to facilitate a vertical PCB. In the OptoZIF Drive, the optical fiber runs parallel to the drive cannula at the distal end, but is bent at the proximal end with the ferrule protruding from a specially designed fiber optic receptacle at a 25 degree angle (figure 1 (e)). This fiber optic receptacle can be modified as needed to support a variety of fiber and ferrule sizes depending on application specific needs. The fiber is placed prior to loading the recording electrodes and the ferrule is fused to the polyimide receptacle using cyanoacrylate adhesive. Bending the fiber in this way may slightly reduce the efficiency of the light transmission, but since large fibers are used (200 microns), and the bending is slight over a few millimeters, the implant has relatively high optical efficiency. The physical coupling process and bending of the fiber resulted in coupling efficiency of approximately 70% from the input fiber to the output of the implant. The optical fiber is positioned so that it just reaches the end of the implant cannula, without extending past and entering the brain. This system facilitates a fiber sitting near the surface of the brain post-implant.

Multi-part protective shell facilitates EMG implantation

The implant contains sensitive electronic, mechanical, and optical components. Thus, for chronic implant experiments, it is important that the implant is properly protected. This is typically accomplished with some form of protective shell surrounding the implant. This shell may also serve a secondary function by incorporating conductive material and providing a conductive path to ground for electromagnetic interference reduction. Previous drives have addressed this shielding/protective function using simple cone shaped shells. Such designs have a large volume compared to the drive itself. Specifically, it extends the lateral boundaries of the drive further past the animal's head which can be unwieldy in behavioral experiments.

To keep the volume of the drive to a minimum while still protecting the internal components, a 3D printed protective shell was created. Initial designs required a protective shell to be installed prior to implantation by sliding the shell over the implant. While meeting the goal of using minimal volume while protecting the implant, it became very difficult to implant EMG electrodes, which must be connected to the EIB during the implant surgery. Thus, the shell was split into two pieces that snap together near the end of the implant procedure and are secured to the drive base with two screws. This enables the EMG electrodes to be implanted, tested, and connected to the EIB without the shell obstructing these steps during the implant surgery. The split shell and drive are shown in figure 1(c).

Two versions of the cap piece to seal the top of the shell are available. The first is used for completely protecting the implant, but cannot be used during recordings. A second cap has an opening that allows the fiber optic cable to be attached as well as the ZIF-clip headstage. During recordings, the drive is covered with a plastic sleeve lined with aluminum foil, which is connected to a ground pin on the drive body to reduce electromagnetic interference during neural recording.

Fixtures and assembly aids speed construction and boosts repeatability

The implant contains a number of small components that must be delicately assembled, often in small batches by users with limited training. The OptoZIF Drive was designed to be assembled quickly over 1-2 days and has a number of additional parts, tools, and guides that have been 3D printed to facilitate rapid and repeatable assembly. On the drive itself, in addition to 3D printing the drive body, the bottom cannula from which the recording electrodes exit has been printed in stainless steel to increase the repeatability of the implant to brain distance and insure a smooth bevel on the distal end.

We also developed additional 3D-printed assembly aids (figure 1(g); supplemental) that allow the implant to be assembled while protecting the most fragile components (i.e. the microwires). The first piece, the holder, keeps the drive affixed and allows the drive to stand-up on its own. This holder is used during the majority of the implant construction process and significantly reduces the probability of accidental damage. The second piece, the pinning fixture, used in combination with the holder, allows gold pins to be “pinned” to the EIB without exerting large forces on the EIB or implant (figure 1(g)).

3D printing of the drive base pieces involves small dimensions and tight tolerances that are near the current technical capabilities of the SLS technology. This is especially a problem for small holes. To address this problem, all holes for steel guide tubes and screws have been purposefully undersized and require clearing by manual drilling. In order to ensure consistent drilling of holes in the base piece, we designed a drill guide that can be 3D printed in stainless steel (figure 1(g)). This drill guide, which fits into grooves on the implant holder to ensure consistent positioning, ensures that the angles of the holes are consistent across drives, and more importantly that the holes for guide tubes and screws are parallel to each other, which is a common source of drive failure.

Finally, we developed a fixture to aid in gold plating recording electrodes. Traditionally, this process had a significant risk of damaging electrodes while lowering the drive into a small well of gold solution (for example using a bench vise or micromanipulator). This fixture consists of two parts, the drive holder in which the implant is secured similar to the holder used during construction, and the base. The base has a small well in the center that is filled with the gold solution with an electrode at the center of the well. The drive holder is then pressed into grooves at the top of the base (after final cutting electrodes to the desired length). This fixture ensures that the electrodes are held at the proper depth to be immersed in the gold solution, but prevents any lateral motion that may damage the electrodes by bringing them into contact with the sides of the well. We have paired this fixture with a breakout interface board that allows easy plating of a specific wire without needing to make electrical contact directly with the ZIF connector or the gold pins on the EIB itself.

Results

To demonstrate the capability of OptoZIF Drive for neural recording and optical feedback, we implanted the drive in mice performing an active sensing task. The OptoZIF drive was implanted over left primary somatosensory cortex, and the EMG electrodes were implanted bilaterally into the facial pad in order to record the muscular activity driving whisker

shows an example of bilateral EMG RMS recordings (*solid black traces*) compared to “gold-standard” whisker angles (*dashed traces*) estimated by manually tracking whisker angles in high speed video (500 frames/sec). We observed here and reported previously that EMG provides a reliable estimate of protraction times, as the EMG signal generally begins increasing prior to an observed increase in whisker angle [32].

The processed EMG was used as a control signal to estimate protraction events in real time and trigger a laser to deliver a single 1 ms pulse of blue light (473 nm, ~35 mW/mm²) to the optical fiber in the implant. Figure 4(b) shows an example trial where stimulation was delivered at EMG estimated protraction times determined by positive crossings of an upper threshold. The system must be reset by a negative crossing of the lower threshold before the next stimulus will be delivered [27]. Stimulation times are indicated by vertical blue bars and show reliable locking to whisker protractions. Importantly, the timing of the stimulus is driven by the motions of the animal, rather than a previously configured choice of stimulation times. Shown along with the EMG is a sample neural recording from SI (bandpassed 0.6-6 kHz). We further demonstrated that similar multiunit responses could be achieved on the same recording channel throughout the duration of the stimulation experiment. Figure 4(c) replicates figure 4(b) with the same recording channel, but on the last stimulated session for this animal (post-implant day 53). Over that duration, stable multiunit responses to whisk-locked stimulation were observed, demonstrating the ability to evaluate responses on a single channel across many sessions.

In order to serve as a robust control signal for real time feedback experiments, EMG recordings must remain stable over a period of many weeks. While much has been done to characterize the stability of tetrode recordings, the stability of EMGs has received less attention. Since EMG electrodes may experience more direct perturbations than intracortical electrodes (e.g. facial grooming), it is important to establish that reliable placement and stable recordings can be achieved. We observed EMG recordings through post-implant day 53 (the last day of data collection for this mouse). Example trials from 5 sessions over that span are shown in figure 5(a). On these trials, the mouse typically begins whisking around 300-500 ms after trial onset. We observed consistent EMG amplitudes and waveform shapes during this period. To quantify the stability of EMG recordings, we evaluated the mean baseline voltage during the first 200 ms of each trial (before significant large amplitude whisking typically begins) within a recording session. Following an initial period of larger variation in baseline voltage corresponding to the initial recovery period, we observed stable baseline voltages for the remainder of the test period (figure 5(b)).

Discussion

The OptoZIF Drive seeks to address a common challenge with rodent recording drives with repositionable electrodes- that they are difficult and time consuming to assemble reliably and consistently, especially by users without specialized training. Small operator errors in conceptually simple operations can result in significant problems later in the construction process and impaired performance in the finished drive. For example, if the holes drilled for the control screws are not parallel to those for the cannula/polyimide/electrode assembly then the ability of the drive to smoothly advance by a repeatable distance with each turn of

the screw will be reduced. We mitigated this specific problem by also 3D printing (in stainless steel) drill guides to ensure accurate and repeatable drilling. In general, we identified steps throughout the construction process that were time consuming and/or vulnerable to operator inconsistencies and developed appropriate assembly tools as needed.

Apart from construction concerns, a major design objective was to limit the height and weight of the implant as much as possible, while still retaining repositionable microdrives. Significant savings in both areas was achieved by incorporating a vertical circuit board to natively support ZIF-clip connections without the use of an adapter. Removing the adapter resulted in a savings of 0.78g and 21 mm. Other design features were targeted specifically towards weight reduction, for example using 3D printed polyimide top pieces to replace metal ones, and incorporating cut-outs in the design of the drive and protective shell to reduce the weight of large features. The result is a low profile drive weighing less than 3 grams and supporting direct connection to TDT headstages.

Although the OptoZIF drive is robust under normal animal behavior, we recommend the standard practice of single housing implanted animals to minimize the potential for damage to the implant or injury to the mouse from cage mates. While there is a tradeoff to removing social interactions, it is extremely difficult to make devices resistant to chewing and other abuse, which would almost certainly impose other complications (e.g. increased weight using harder materials). Moreover, implanted animals would remain at risk for injury, e.g. at skin margins, regardless of the device design. While we designed the OptoZIF drive around the size requirements of mouse implants, there is no reason in principle why it could not be used for recordings in rats for applications requiring a particularly small, light-weight recording drive. Additional support screws placed in the skull would typically be used to offset higher contact forces, but the drive materials themselves should be sufficient to maintain drive integrity.

Open loop stimulation experiments that perturb a system and observe the output on neural activity and/or behavior have been a staple of neuroscience labs for decades. It is becoming increasingly apparent, however, that closed loop stimulation paradigms offer a powerful method to study circuits in which the brain integrates information in real time while coordinating future outputs. The ability to record a control signal (EMG), process it in real time, and deliver real-time feedback while simultaneously recording neural activity from 6 tetrodes (24 wires) demonstrates the power of OptoZIF Drive for closed-loop stimulation experiments. Similarly, many neuroscience experiments have isolated particular aspects of a target system for study (i.e. anesthetized preps, head fixation, and whisker trimming in the rodent whisker system). The importance of experiments that allow for more natural behaviors is also becoming clear [28]. By incorporating the ability to easily perform closed-loop stimulation experiments within a drive that has been engineered to accommodate more natural behaviors (i.e. weight reduction and lower profile), OptoZIF Drive provides an excellent platform to study a range of relevant neuroscience question in mice.

The OptoZIF Drive is the first optical stimulation capable drive design that supports adapter-free interfacing with the ZIF-clip system. The innovative drive design, along with the associated fixtures and guides to aid in repeatable assembly represent an important step

forward. Validation of OptoZIF Drive in a real time feedback experiment delivering stimulation timed to whisker motions demonstrates the drive's utility for closed loop experiments in freely moving animals.

Supplementary Material

Refer to Web version on PubMed Central for supplementary material.

Acknowledgements

J.B.S. was supported by a Quantitative Biology and Physiology Training Program (NIH 5 T32 GM 8764-10). J.T.R. holds a Career Award at the Scientific Interface from the Burroughs Wellcome Fund. Pilot funding for implant design was contributed by the Boston University Center for Neuroscience.

References

1. Aravanis AM, Wang L-P, Zhang F, Meltzer LA, Mogri MZ, Schneider MB, Deisseroth K. An optical neural interface: in vivo control of rodent motor cortex with integrated fiberoptic and optogenetic technology. *J. Neural Eng.* 2007; 4:S143–56.
2. Boyden ES, Zhang F, Bamberg E, Nagel G, Deisseroth K. Millisecond-timescale, genetically targeted optical control of neural activity. *Nat. Neurosci.* 2005; 8:1263–8. [PubMed: 16116447]
3. Madisen L, Mao T, Koch H, Zhuo J, Berenyi A, Fujisawa S, Hsu Y-WA, Iii AJG, Gu X, Zanella S, Kidney J, Gu H, Mao Y, Hooks BM, Boyden ES, Buzsáki G, Ramirez JM, Jones AR, Svoboda K, Han X, Turner EE, Zeng H. A toolbox of Cre-dependent optogenetic transgenic mice for light-induced activation and silencing. *Nat. Neurosci.* 2012; 15:793–802. [PubMed: 22446880]
4. Zhang F, Wang L-P, Brauner M, Liewald JF, Kay K, Watzke N, Wood PG, Bamberg E, Nagel G, Gottschalk A, Deisseroth K. Multimodal fast optical interrogation of neural circuitry. *Nature.* 2007; 446:633–9. [PubMed: 17410168]
5. Zhang F, Gradinaru V, Adamantidis AR, Durand R, Airan RD, de Lecea L, Deisseroth K. Optogenetic interrogation of neural circuits: technology for probing mammalian brain structures. *Nat Protoc.* 2010; 5:439–56. [PubMed: 20203662]
6. McNaughton BL, O'Keefe J, Barnes CA. The stereotrode: a new technique for simultaneous isolation of several single units in the central nervous system from multiple unit records. *J. Neurosci. Methods.* 1983; 8:391–7. [PubMed: 6621101]
7. Gray CM, Maldonado PE, Wilson M, McNaughton B. Tetrodes markedly improve the reliability and yield of multiple single-unit isolation from multi-unit recordings in cat striate cortex. *J. Neurosci. Methods.* 1995; 63:43–54. [PubMed: 8788047]
8. Kloosterman F, Davidson TJ, Gomperts SN, Layton SP, Hale G, Nguyen DP, Wilson MA. Micro-drive Array for Chronic in vivo Recording: Drive Fabrication. *J. Vis. Exp.* 2009
9. Nguyen DP, Layton SP, Hale G, Gomperts SN, Davidson TJ, Kloosterman F, Wilson MA. Micro-drive Array for Chronic in vivo Recording: Tetrode Assembly. *J. Vis. Exp.* 2009
10. Siegle JH, Carlen M, Meletis K, Tsai L-H, Moore CI, Ritt J. Chronically implanted hyperdrive for cortical recording and optogenetic control in behaving mice. *Engineering in Medicine and Biology Society, EMBC, 2011 Annual International Conference of the IEEE.* 2011:7529–32.
11. Voigts J, Siegle JH, Pritchett DL, Moore CI. The flexDrive: an ultra-light implant for optical control and highly parallel chronic recording of neuronal ensembles in freely moving mice. *Front. Syst. Neurosci.* 2013; 7
12. Brunetti PM, Wimmer RD, Liang L, Siegle JH, Voigts J, Wilson M, Halassa MM. Design and Fabrication of Ultralight Weight, Adjustable Multi-electrode Probes for Electrophysiological Recordings in Mice. *J. Vis. Exp.* 2014
13. Chang EH, Frattini SA, Robbiati S, Huerta PT. Construction of Microdrive Arrays for Chronic Neural Recordings in Awake Behaving Mice. *J. Vis. Exp.* 2013

14. Fee MS, Leonardo A. Miniature motorized microdrive and commutator system for chronic neural recording in small animals. *J. Neurosci. Methods*. 2001; 112:83–94. [PubMed: 11716944]
15. Jackson N, Sridharan A, Anand S, Baker M, Okandan M, Muthuswamy J. Long-Term Neural Recordings Using MEMS Based Movable Microelectrodes in the Brain. *Front. Neuroengineering*. 2010; 3
16. Yamamoto J, Wilson MA. Large-Scale Chronically Implantable Precision Motorized Microdrive Array for Freely Behaving. *Animals J. Neurophysiol*. 2008; 100:2430–40. [PubMed: 18667539]
17. Yang S, Cho J, Lee S, Park K, Kim J, Huh Y, Yoon E-S, Shin H-S. Feedback controlled piezo-motor microdrive for accurate electrode positioning in chronic single unit recording in behaving mice. *J. Neurosci. Methods*. 2011; 195:117–27. [PubMed: 20868709]
18. Anikeeva P, Andalman AS, Witten I, Warden M, Goshen I, Grosenick L, Gunaydin LA, Frank LM, Deisseroth K. Optetrode: a multichannel readout for optogenetic control in freely moving mice. *Nat. Neurosci*. 2011; 15:163–70. [PubMed: 22138641]
19. Ozden I, Wang J, Lu Y, May T, Lee J, Goo W, O'Shea DJ, Kalanithi P, Diester I, Diagne M, Deisseroth K, Shenoy KV, Nurmikko AV. A Coaxial Optrode As Multifunction Write-Read Probe for Optogenetic Studies in Non-Human Primates. *J. Neurosci. Methods*. 2013; 219:142–54. [PubMed: 23867081]
20. Royer S, Zemelman BV, Barbic M, Losonczy A, Buzsáki G, Magee JC. Multi-array silicon probes with integrated optical fibers: light-assisted perturbation and recording of local neural circuits in the behaving animal. *Eur. J. Neurosci*. 2010; 31:2279–91. [PubMed: 20529127]
21. Lee J, Ozden I, Song Y-K, Nurmikko AV. Transparent intracortical microprobe array for simultaneous spatiotemporal optical stimulation and multichannel electrical recording. *Nat. Methods*. 2015; 12:1157–62. [PubMed: 26457862]
22. Wang J, Wagner F, Borton DA, Zhang J, Ozden I, Burwell RD, Nurmikko AV, van Wagenen R, Diester I, Deisseroth K. Integrated device for combined optical neuromodulation and electrical recording for chronic in vivo applications. *J. Neural Eng*. 2011; 9:016001. [PubMed: 22156042]
23. McAlinden N, Gu E, Dawson MD, Sakata S, Mathieson K. Optogenetic activation of neocortical neurons in vivo with a sapphire-based micro-scale LED probe. *Front. Neural Circuits*. 2015; 9
24. Lin L, Chen G, Xie K, Zaia KA, Zhang S, Tsien JZ. Large-scale neural ensemble recording in the brains of freely behaving mice. *J. Neurosci. Methods*. 2006; 155:28–38. [PubMed: 16554093]
25. Fan D, Rich D, Holtzman T, Ruther P, Dalley JW, Lopez A, Rossi MA, Barter JW, Salas-Meza D, Herwik S, Holzhammer T, Morizio J, Yin HH. A Wireless Multi-Channel Recording System for Freely Behaving Mice and Rats. *PLoS ONE*. 2011; 6
26. Wentz CT, Bernstein JG, Monahan P, Guerra A, Rodriguez A, Boyden ES. A wirelessly powered and controlled device for optical neural control of freely-behaving animals. *J. Neural Eng*. 2011; 8:046021. [PubMed: 21701058]
27. Schroeder JB, Mariano VJ, Telian GI, Ritt JT. Stimulation of somatosensory cortex locked to whisker motions in a mouse model of active sensing. 2013 6th International IEEE/EMBS Conference on Neural Engineering (NER) 2013 6th International IEEE/EMBS Conference on Neural Engineering (NER). 2013:637–40.
28. Schroeder JB, Ritt JT. Selection of Head and Whisker Coordination Strategies During Goal Oriented Active Touch. *J. Neurophysiol*. 2016;jn.00465.2015.
29. Arenkiel BR, Peca J, Davison IG, Feliciano C, Deisseroth K, Augustine GJ, Ehlers MD, Feng G. In Vivo Light-Induced Activation of Neural Circuitry in Transgenic Mice Expressing Channelrhodopsin-2. *Neuron*. 2007; 54:205–18. [PubMed: 17442243]
30. Fenno L, Yizhar O, Deisseroth K. The Development and Application of Optogenetics. *Annu. Rev. Neurosci*. 2011; 34:389–412. [PubMed: 21692661]
31. Hippenmeyer S, Vrieseling E, Sigrist M, Portmann T, Laengle C, Ladle DR, Arber S. A developmental switch in the response of DRG neurons to ETS transcription factor signaling. *PLoS Biol*. 2005; 3:e159. [PubMed: 15836427]
32. Schroeder JB, Ritt JT. Extraction of intended palpation times from facial EMGs in a mouse model of active sensing. 2013 35th Annual International Conference of the IEEE Engineering in Medicine and Biology Society (EMBC) 2013 35th Annual International Conference of the IEEE Engineering in Medicine and Biology Society (EMBC). 2013:2016–9.

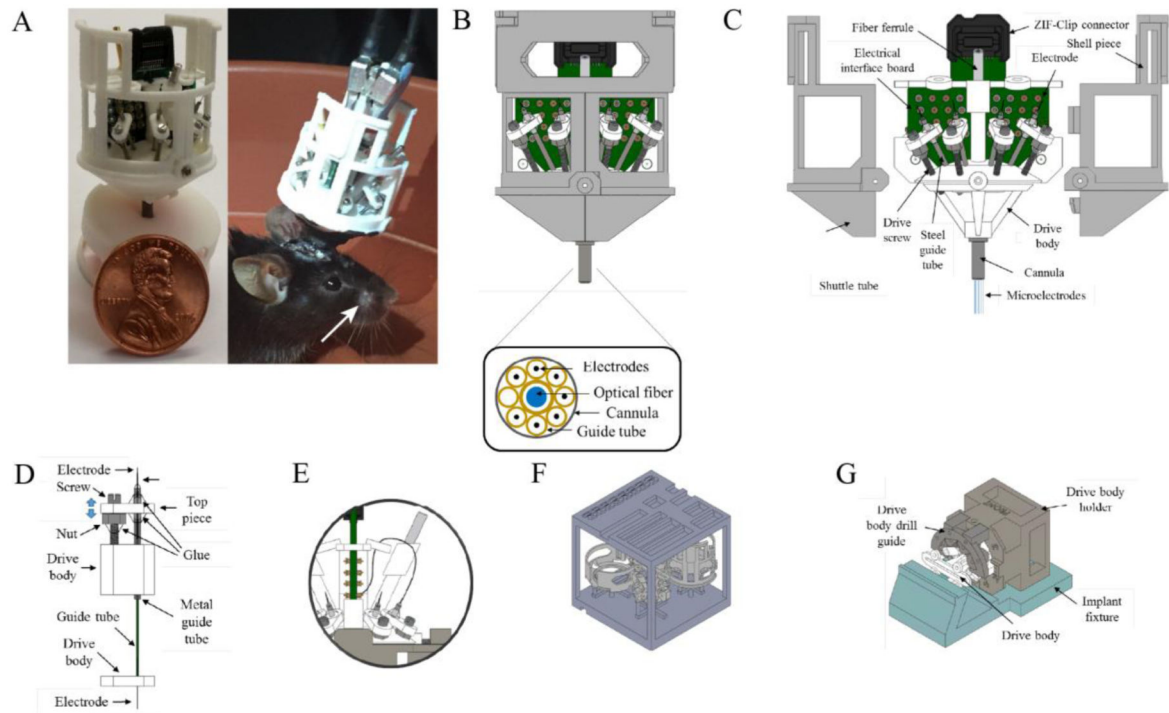


Figure 1. Assembled OptoZIF-Drive with component detail

A) Photo of OptoZIF Drive with scale reference (*left*) and implanted mouse showing OptoZIF Drive with the fiber and protective shell removed for visibility (*right*). White arrow indicates approximate location of EMG electrode implants. **B)** Assembled OptoZIF Drive with protective shell and cap attached. *Inset*- Arrangement of guide tubes and optical fiber in cannula. **C)** Exploded view of drive with components labeled. **D)** Drive mechanism for positioning microelectrodes. **E)** Zoomed drive image highlights the angled optical fiber receptacle and microelectrode wiring method. **F)** Main 3D printed “block” of OptoZIF drive body and parts. **G)** Assembly aids include a drive holder, a drill guide, and an implant fixture for connecting microelectrodes to EIB.

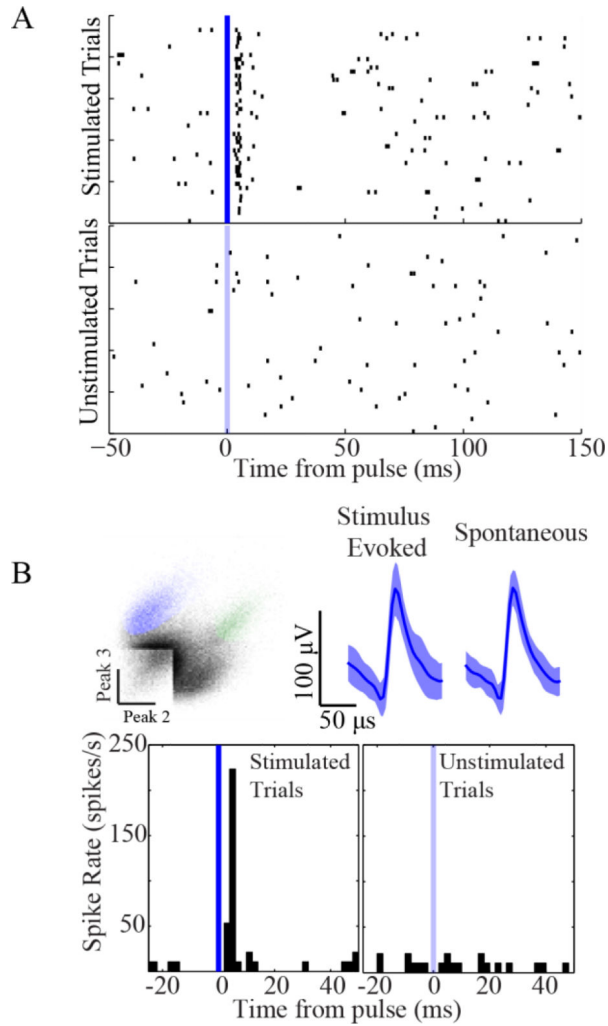


Figure 2. Multi Unit and Single Unit responses to optogenetic cortical stimulation
A) Rasters of multiunit spiking for SI recordings bandpassed (0.6-6 kHz) and thresholded to find spike times (5 std. above mean threshold) during real time feedback stimulation locked to whisker motions. Stimulation pulses (top) show a robust recruitment of multiunit spiking ~5 ms after pulse onset compared to unstimulated trials (bottom) when the signal processing was identical but no output was delivered to the laser. **B)** Clusters for a sample tetrode recording from SI. Waveforms for stimulus evoked (top-middle) and spontaneous (top-right) spikes demonstrate that SI stimulation is recruiting SI activity comparable to naturally occurring. PSTHs for a single isolated unit in SI (blue cluster above) in response to the same stimulation conditions as A. Stimulation (bottom-left) produces a reliable increase in firing of this unit compared to the mock pulse condition (bottom-right).

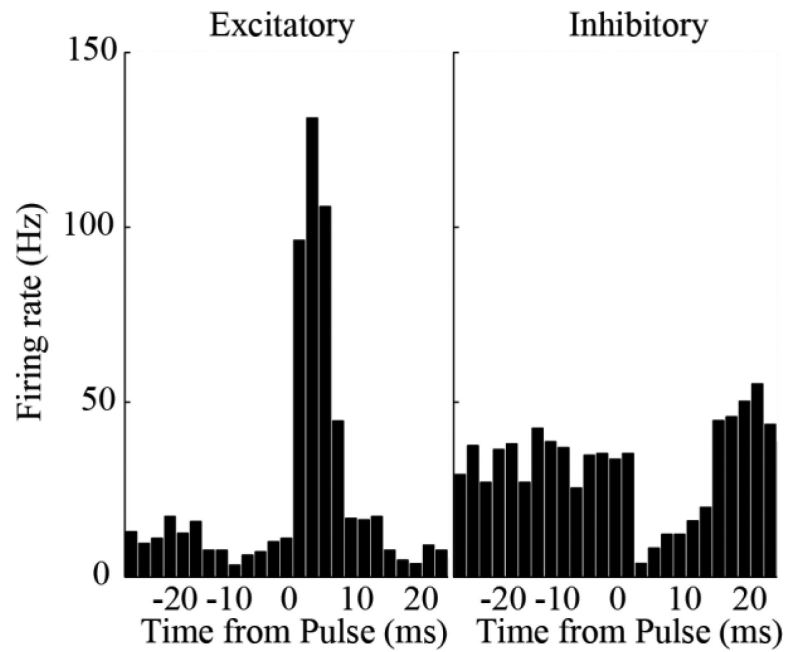


Figure 3. Opposite effects observed for excitatory vs. inhibitory stimulation

Single 1 ms pulses were delivered at random times drawn from a Poisson distribution on a subset of trials within each session. Multiunit SI activity from one channel on each tetrode was averaged across all stimulated sessions for an animal expressing ChR2 in excitatory cells (left) and one expressing ChR2 in inhibitory interneurons (right). The pronounced difference in direction of effect for these two types of mice is not consistent with misidentification of stimulation artifacts as unit activity.

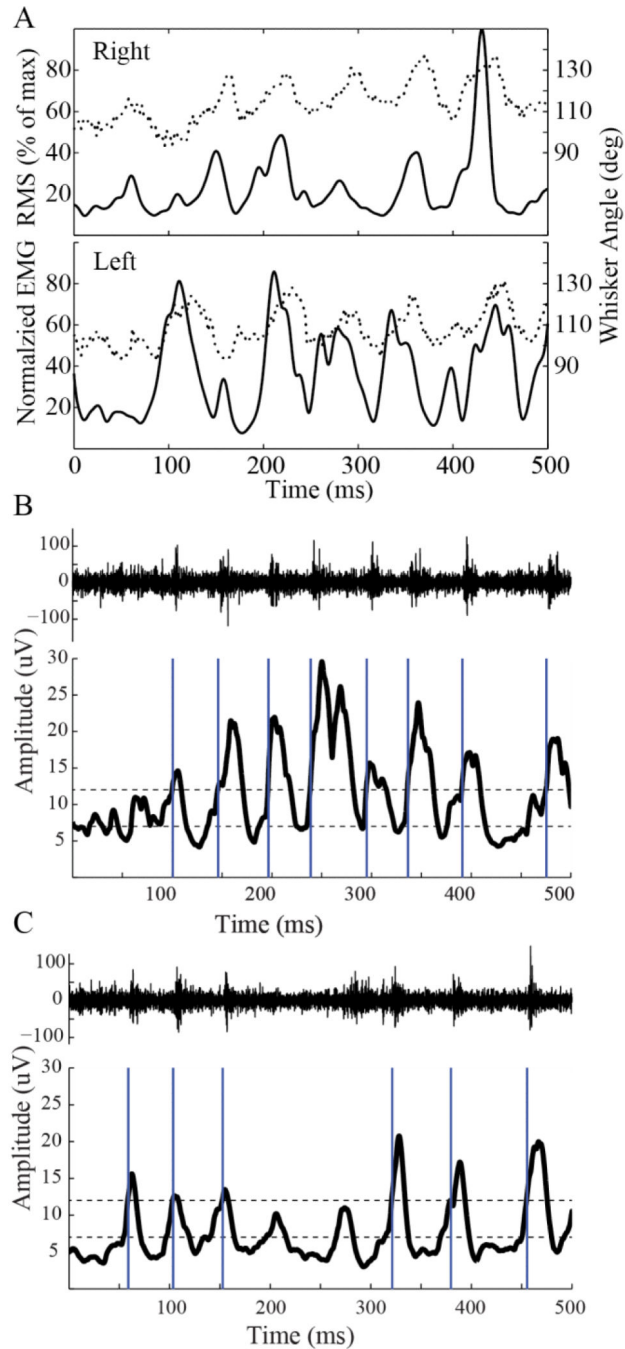


Figure 4. Facial Electromyography tracks whisker motions and drives real time feedback stimulation

A) Right (top) and left (bottom) EMG signals were processed offline to compute the signal RMS (solid traces) and compared to videographically reconstructed whisker angles (dashed traces). The comparison shows that EMG provides a reliable estimate of whisker timing, particularly an indication of protraction onsets, and verifies its utility as a control signal for real time feedback stimulation. **B)** An example trial shows optogenetic stimulation of SI (blue bars) timed to whisker motions using EMG (bottom, black trace). A sample recording from SI (top) (bandpassed 0.6-6 kHz) shows robust multiunit activation timed to stimulation.

C) An example trial from the same recording channel as **B** but on the last stimulated session (post implant day 53) demonstrates comparable, stable responses over the duration of the experiment.

Author Manuscript

Author Manuscript

Author Manuscript

Author Manuscript

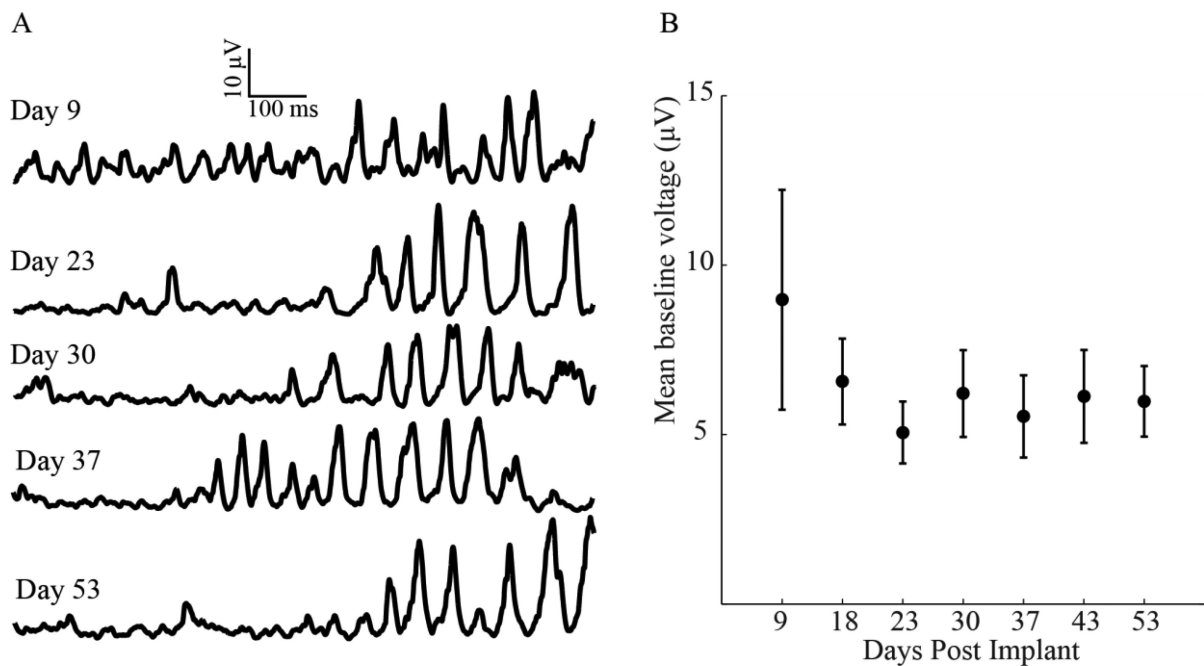


Figure 5. EMG provides a stable control signal

A) EMG recordings examples trials from 5 sessions between post-implant days 9 and 53. Whisking typically begins 300-500 ms after trial initiation and consistent amplitudes and waveforms are overserved throughout the recording period. **B)** The mean baseline voltage (average EMG potential in the first 200ms of each trial in a session) shows stability after an initial period of high variation (during post-surgical recovery, prior to data collection) (mean \pm std).